applied sciences

MDPI

Article

Mixtures of Cationic Linear Polymer and Anionic Polymeric Microspheres for Stabilization of Sand: Physicochemical, Structural and Mechanical Study

Irina Panova [1,*], Evgeniya Shevaleva [2], Inessa Gritskova [2], Maxim Arzhakov [1] and Alexander Yaroslavov [1]

[1] Faculty of Chemistry, Lomonosov Moscow State University, 119991 Moscow, Russia
[2] Department of Chemistry and Technology of Macromolecular Compounds, MIREA—Russian Technological University, 119571 Moscow, Russia
* Correspondence: igpan@mail.ru

Abstract: Aqueous formulations based on anionic butadiene-styrene microspheres (BSMs) and cationic poly(diallyldimethylammonium chloride) (PDADMAC) with the weight PDADMAC fraction from 0 to 1 were studied as the stabilizers of loose sandy soils. In general, these systems were shown to be represented as the mixtures of microspheres saturated with PDADMAC and unbound polycation. Mechanical testing of BSMs–PDADMAC films evidenced that with increasing weight PDADMAC fraction, a 20-fold growth in elastic modulus, 2-fold growth in strength and 2-fold decrease in ultimate strain of the material were observed. Treatment of the sand with the above formulations resulted in formation of a protective porous polymer-sand surface crust with the strength from 0.8 to 45.0 MPa. "Elasticity–rigidity" balance and water resistance of the crusts were controlled by weight fraction of polycation in the mixed formulation. Stable water-resistant polymer-sand crusts were shown to be prepared using formulations with the weight PDADMAC fraction from 0 to 0.2. The results indicated a great potential of the polymer-colloid formulations for the fabrication of structured sand coatings with controlled properties.

Keywords: anionic polymer microspheres; linear polycation; saturated complex; sand; polymer-sand coatings; elasticity; strength; water resistance

Citation: Panova, I.; Shevaleva, E.; Gritskova, I.; Arzhakov, M.; Yaroslavov, A. Mixtures of Cationic Linear Polymer and Anionic Polymeric Microspheres for Stabilization of Sand: Physicochemical, Structural and Mechanical Study. *Appl. Sci.* **2023**, *13*, 4311. https://doi.org/10.3390/app13074311

Academic Editor: Antonino Pollicino

Received: 18 February 2023
Revised: 15 March 2023
Accepted: 22 March 2023
Published: 28 March 2023

1. Introduction

At the present time, synthetic polymers are widely used as engineering materials in the construction industry and agriculture [1–3]. These areas include the creation of building elements [4,5], the modification of concrete and mortars [6,7], and the coating of roads and highways [8,9]. Polymers were shown to prevent soil erosion [3,10–12], conserve waste rocks on mining enterprises [13,14], localize contaminated disperse systems such as silt and ash [15,16], reinforce highways and railways slopes, earthen dams and embankments [17–19], and fix loose soils, primarily sands [20–23]. This range of applications is based on the polymer ability to bind mineral and organo-mineral particles to larger aggregates or a monolithic body. The growing contribution of polymers to solve the above problems is associated with the fact that traditional binders and additives (Portland cement, slaked lime, bitumen, microsilica, etc.) [24–26] seem to be not sufficiently friendly from the ecological viewpoint. Their production is accompanied by significant emissions of carbon dioxide and nitrogen oxides into the atmosphere [27]. In connection with this, polymeric binders such as urea-formaldehyde resins, polyvinyl acetate, polyvinyl alcohol, polyacrylamide, and polyurethanes are successfully introduced into practice [28–33].

As for the soil or ground treatment, two basic methods are recognized: mixing of aqueous polymer formulation with the substrate [34] and deposition of the formulations over the substrate surface [35]. In the first case, the polymers were mixed with the soil and distributed to a depth of up to 30 cm. The stabilizing effect is achieved at a polymer

consumption of several tons per hectare; natural polymers, i.e., polysaccharides, quickly decomposed when introduced into the soil and ceased to work as stabilizers. The replacement of natural polymers with synthetic ones allowed to eliminate the problem of polymer degradation, but did not lead to a decrease in the consumption of polymers. In the second case, deposition of an aqueous polymer formulation resulted in a sharp reduction in the consumption of polymers, which now formed a rather thin protective polymer-soil surface layer, typically ca. 5 mm deep, which prevented mechanical destruction of soil and its erosion with water and wind [36,37]. The stabilization was due to inter-particle binding or "physical crosslinking" of particles with polymers and the formation of continuous protective coatings [38,39].

Recently, interpolyelectrolyte complexes (IPEC) were proposed as promising soil ameliorants [11,40]. IPEC are the products of electrostatic interaction between two oppositely charged ionic polymers (polyelectrolytes, PEs) [41]. Variation of the IPEC composition allows one to adjust the structure and control the mechanical properties and erosion resistance of the soil-IPEC protective coatings [11]. The IPECs based on linear ionic polymers ensure an acceptable mechanical stability of the coatings [11,42,43], their moisture and air permeability [11], and a stimulating effect on the germination and development of plants [11,44]. However, these coatings are characterized by rather high rigidity that restricts their application, for example, when fixing the area with the complicated relief configuration. The elasticity of the coating can be improved using latexes—aqueous suspensions of the rubbery polymeric microspheres [45,46].

To summarize, polymer-soil protective coatings require desired mechanical properties associated with the controlled rigidity–elasticity balance and high water and wind resistance. To advance in this problem, the polymer-colloid mixtures of rubbery latexes and rigid IPECs seem to be the most promising formulations.

In this article, the complexation of anionic butadiene-styrene microspheres and cationic linear poly(diallyldimethylammonium chloride) (PDADMAC) and mechanical behavior of the resulting microsphere/PDADMAC binary films are described. This information is used for setting experiments on the deposition of the polymer formulation over sand, interpretation of the composition–properties relationship for the protective polymer-sand coatings and discussion of prospects for the use of polymer-colloid binary formulations as a non-structured sand binder.

It should be noted that in our research non-biodegradable butadiene-styrene microspheres and PDADMAC were used. At the same time, synthetic ionic polymers were shown to demonstrate a negligible toxicity towards soil microorganisms and higher plants after these polymers bind to organic and mineral particles [44]. It other words, the synthetic polymers are compatible with the soil environment. From this point of view, ionic polymers are as safe for the soil as conventional soil conditioners, e.g., polyacrylamide.

2. Experimental

2.1. Materials

Butadiene-styrene latex (BSL) (OJSC, Voronezhsintezkauchuk, Voronezh, Russia) with 50 wt.% of carboxylated butadiene-styrene microspheres (BSMs) with diameter of 100 nm, PDADMAC with M_w = 200–350 kDa (Sigma-Aldrich, St. Louis, MO, USA) and fine-grained quartz sand with a grain size of 0.5–1 mm (ORT6, Russia) were used.

The concentration of BSM carboxyl groups estimated by conductometric titration of latex using a CDM 83 conductivity meter (Radiometer, Copenhagen, Denmark) was 0.06 mol per 1 g of BSMs. Before testing the quartz sand, it was repeatedly rinsed with bi-distilled water and dried.

Mixed BSM/PDADMAC compositions with different polymer-to-polymer ratios were prepared via addition of a polycation solution to the latex suspension followed by vigorous stirring. The pH of PDADMAC solution and BSM suspension was pre-adjusted to pH 7. The concentration of polymers was expressed in moles of ionic groups of polymers per liter: cationic for PDADMAC and anionic for BSM.

2.2. Methods

For aqueous solutions and suspensions, the values of pH were measured using a Corning 340 pH meter (Corning, NY, USA) equipped with a combined glass pH electrode.

The electrophoretic mobility (EPM) of dispersed particles was studied using a Brookhaven Zeta Plus (Holtsville, NY, USA) at 22 °C. Their average hydrodynamic diameter was measured by dynamic light scattering at a fixed scattering angle (90°) in a thermostatic cell. The diameter of particles was calculated using the DynaLS software (version 2.7.1. (Alango Ltd., Newlands West, South Africa)).

For mechanical testing, BSL-PDADMAC films with a thickness of 0.2 ± 0.02 mm were prepared via deposition of the 4 wt.% polymer formulation on a cellophane substrate. The films were dried at room temperature at the humidity of 30% for 5 days and removed from the substrate. Dog-bone testing samples with the working part of 6 × 20 mm^2 were uniaxially drawn at room temperature with a strain rate of 1.4 × 10^{-2} s^{-1} using Instron-4301 (Norwood, MA, USA). Young's modulus E_0 was estimated as the slope of the initial linear portion of σ-ε diagrams with an accuracy of ±7%. An accuracy of estimation of the strength σ_f and ultimate strain ε_f was ±7% and ±10%, respectively.

For mechanical testing, protective polymer-sand coatings (polymer-sand crusts) were prepared as follows. In a plastic dish, the sand layer with the thickness of 5 cm and the surface area of 20 cm^2 was formed using 160 g of the sand. After that, a 1 wt.% aqueous polymer formulation was deposited over the sand layer with a consumption rate of 2 L/m^2. As-prepared samples were dried for a week at room temperature at 30% humidity. The strength of the coatings was measured by a plastic deformation method using a Rebinder conical plastometer (Soil Science Department, Lomonosov Moscow State University) [47]. The samples were loaded with a metal cone until the cracking of the coating surface. The force causing the fracture of the crust was recalculated to pressure, that is, the strength of material P_f.

To study the erosion stability of the sand layers, 100 g of sand were placed on a Petri dish to form the layer with a thickness of 1 cm and surface area of 80 cm^2. The sand was coated with a 1 wt.% polymer aqueous formulation with a rate of consumption of 2 L/m^2. As-prepared samples were dried to a constant weight at 22 °C and a humidity of 30%. Petri dishes were placed at the angle of 45° and treated with 200 mL of water from a spray gun in a pulsed mode for 10 min. After drying, the weight loss was calculated.

The morphology of polymer-sand coatings was studied with a JEOL JSM-6380LA scanning electron microscope (Akishima, Japan). The initial coatings as well as coatings prepared via brittle fracturing in liquid nitrogen were used. The images were obtained in the electron microscopy laboratory of Lomonosov Moscow State University Biology Department.

All experiments were performed with 3–5 repetitions. Statistical data processing was carried out with the Excel program; the confidence interval was 95%.

3. Results and Discussion

3.1. Formation of BSM–PDADCAC Binary Formulations

In aqueous medium, carboxylated BSMs are negatively charged. An electrostatic interaction of these microspheres with positively charged PDADMAC results in the formation of the polymer-colloid PDADMAC–BSM complexes. The regularities of complexation were revealed via the study of EPM of resulting PDADMAC–BSM particles.

Figure 1 shows the dependence of EPM on the ratio between a mole concentration of quaternized PDADMAC groups and a mole concentration of carboxylic BSMs groups, $Z = [N^+]/[COO^-]$. Injection of a PDADMAC aqueous solution into a BSL resulted in the adsorption of PDADMAC macromolecules on the microsphere surface, decreasing the negative charge of the particles followed by their complete neutralization at EPM = 0.

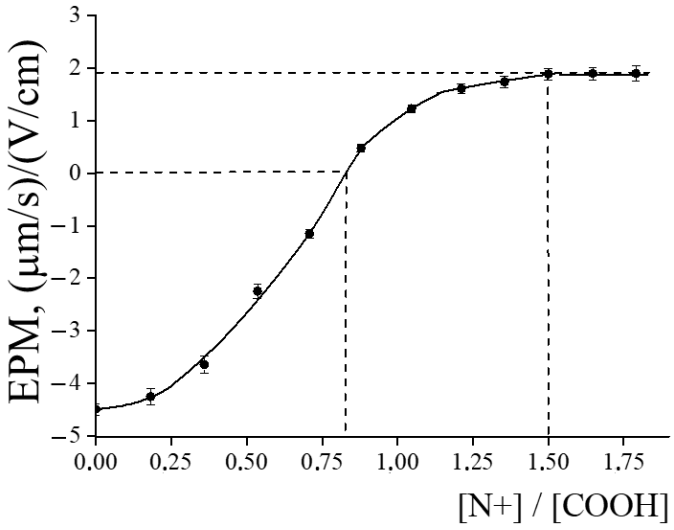

Figure 1. Electrophoretic mobility of BSM–PDADMAC complex particles vs. Z. [BSM] = 4×10^{-5} M; 0.01 M phosphate buffer with pH 7.

The composition of the electro-neutral PDADMAC–BSM complex was determined using an earlier described approach [48,49] based on the two main points. At first, positively charged groups of cationic PDADMAC interact completely with negatively charged carboxyl groups at anionic BSMs. As a result, all polycation chains are bound by latex particles, and their surface is completely covered by the polymer. Second, at the EPM = 0, a concentration of the positive PDADMAC groups, involved in the complexation ($[N^+]_{EPM = 0}$), is equal to the concentration of the negative (ionized) BSM groups ($[COO^-]_{EPM = 0}$). These ideas allowed the composition of an electro-neutral complex $Z_0 = [N+]_{EPM = 0}/[COOH]_{EPM = 0} = 0.82$. A degree of dissociation of the surface carboxylic groups at pH 7 is of $\alpha \approx 0.7$ [50]. Extra ionized COO^- groups (≈0.1) were involved in complexation due to a cooperative displacement of protons from carboxylic BSM groups by the interacting PDADMAC [41]. Non-dissociated carboxylic BSM groups, whose fraction was 0.18, did not form ionic bridges with the cationic PDADMAC. The composition of the PDADMAC–BSM complex can be re-calculated in terms of the weight fraction of PDADMAC as $W = W_{PDDAMAC}/(W_{BSM} + W_{PDADMAC})$, where $W_{PDDAMAC}$ and W_{BSM} are current weights of PDADMAC and BSM, respectively. For the electro-neutral complex, we get $W_0 = W_{PDAMAC(EPM = 0)}/(W_{BSM(EPM = 0)} + W_{PDADMAC(EPM = o)}) = 0.02$, where $W_{PDAMAC(EPM = 0)}$ and $W_{BSM(EPM = 0)}$ are weights of both components at EPM = 0. The increase in Z was accompanied by the additional binding of PDADMAC and an appearance of the positive charge on the BSM surface. The ultimate positive EPM value was +2 (μm/s)/(V/cm) and did not change with the further growth in Z. This EPM value corresponded to the maximum adsorption of PDADMAC onto the surface of negative BSMs and the formation of the saturated PDADMAC–BSM complex [49,51,52]. The positive charge stabilized the saturated complex particles against aggregation; their size was close to 170 nm as compared with 100 nm for the virgin BSM. Note, the saturation takes place at $Z_{sat} = 1.5$ (see Figure 1) or $W_{sat} = 0.036$. At $W > W_{sat}$, an accumulation of unbound PDADMAC is observed, and the PDADMAC–BSM binary mixture contains the saturated PDADMAC–BSM complex and unbound PDADMAC. From this standpoint, the weight fraction of PDADMAC W can be considered as the key parameter which describes the composition of the PDADMAC–BSM formulations.

3.2. Mechanical Properties of BSMs–PDADMAC Films

The results discussed in the previous section provide evidence that the weight fraction of PDADMAC W has the marked influence on the composition and structural features of resulting PDADMAC–BSM systems. The formulation with W = 0 is represented as a stable aqueous suspension of negatively charged BSMs. The formulation with W = 0.036 corresponds to a stable aqueous suspension of saturated positively charged PDADMAC–

BSM complex particles. At 0.036 < W < 1, the formulation is considered as the mixture of the saturated complex particles and unbound PDADMAC. At W = 1, the formulation is an aqueous solution of the virgin PDADMAC. To study the influence of the composition of PDADMAC–BSM samples on their mechanical properties, the films prepared from the binary PDADMAC–BSM mixtures were tested. Note that BSMs are characterized by a well-pronounced ability for film formation, whereas PDADMAC is not prone to do it. For this reason, a PDADMAC content in the binary mixtures W was varied from 0 to 0.5. Figure 2 shows stress–strain diagrams for several typical films prepared from BSMs with W = 0 (curve 1) and PDADMAC–BSM mixtures with different W (curves 4–8). For all samples studied (nine in total), mechanical characteristics are listed in Table 1 (columns 3–5). The numbers at the curves in Figure 2 correspond to the sample numbers in Table 1.

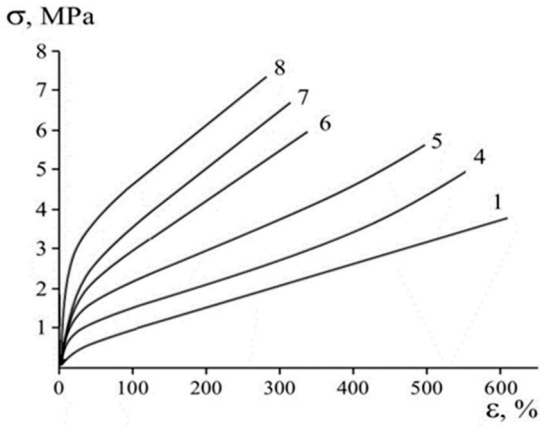

Figure 2. Stress–strain diagrams for the films prepared from BSL (W = 0) (1) and BSMs–PDADMAC mixtures with W = 0.077 (4), 0.111 (5), 0.2 (6), 0.333 (7) and 0.5 (8). Numbers at the curves correspond to the sample numbers in Table 1.

Table 1. Mechanical properties of BSMs–PDADMAC films and polymer-sand crusts with different PDADMAC content W.

No.	W	PDADMAC-BSM Films			Strength of Polymer-Sand Crust P_f, MPa
		Elastic Modulus (E_0), mPa	Strength (σ_f), mPa	Ultimate Strain (ε_f), %	
1	2	3	4	5	6
1	0	4.5 ± 0.4	3.5 ± 0.3	580 ± 60	0.8
2	0.036	5.0 ± 0.4	3.8 ± 0.3	570 ± 55	1.1
3	0.059	5.5 ± 0.45	4.0 ± 0.3	560 ± 55	1.9
4	0.077	9.0 ± 0.65	5.05 ± 0.25	550 ± 55	2.7
5	0.111	11.0 ± 0.8	5.5 ± 0.15	480 ± 50	3.5
6	0.2	15.0 ± 1.0	5.7 ± 0.2	330 ± 45	8.0
7	0.33	17.0 ± 2.0	6.6 ± 0.25	300 ± 40	13.0
8	0.5	90.0 ± 8.0	7.2 ± 0.4	270 ± 20	18.0
9	1	-	-	-	45.0

As follows from the data in Table 1, the growth in W or increasing PDADMAC content in the mixture results in noticeable changes in the mechanical characteristics of BSMs–PDADMAC films—a 20-fold increase in elastic modulus, 2-fold increase in the strength, and 2-fold decrease in the ultimate strain of the samples. Thus, the addition of the inelastic hydrophilic PDADMAC to the elastic BSMs is accompanied by the growth in rigidity of the films and decrease in their elasticity. In other words, the variation of PDADMAC content in a BSMs–PDADMAC formulation allows one to control the rigidity–elasticity balance of the final material. For a more detailed analysis of this effect, let us consider the dependences of the mechanical properties of the films on PDADMAC content W.

Figure 3 shows the dependences of elastic modulus E_0 and ultimate strain on W. Note that both curves are characterized by well-pronounced inflection at PDADMAC content

W_{in} in the range from 0.04 to 0.06. Within the interval $0 < W < W_{in}$, increasing PDADMAC content has no noticeable influence on the elastic modulus and ultimate strain of BSMs–PDADMAC films. With the further increase in W, marked growth in E_0 takes place whereas ε_f falls down. For $\sigma_f = f(W)$ plot, the behavior similar to that for $E_0 = f(W)$ was observed (data are not shown). The W_{in} value (0.04–0.06) is in a good agreement with the value of W_{sat} = 0.036, at which the saturation of the BSMs–PDADMAC complex takes place. Thus, a transition from the negative charge in the BSMs system to the positive charge in the saturated BSMs–PDADMAC complex has a negligible effect on the mechanical properties of the films. In both cases, the properties are determined by the BSM component, whose weight content remains practically constant and close to the maximum (0.96–1). A sharp growth in the rigidity of BSMs–PDADMAC films (increasing elastic modulus and strength and decreasing ultimate strain) is controlled by accumulation of unbound polycation in the formulation when PDADMAC content exceeds the W_{sat} value.

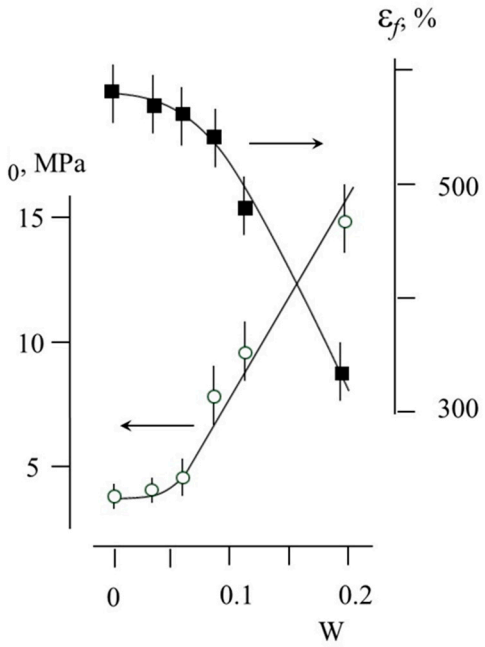

Figure 3. Dependence of elastic modulus E_0 and ultimate strain ε_f of BSMs–PDADMAC films on the weight fraction of PDADMAC in formulation W.

3.3. Structure and Properties of Polymer-Sand Protective Coatings

The treatment of quartz sand with the above formulations was carried out according to a procedure discussed in [43] to form a protective soil coating. The preparation of polymer-sand coatings involved deposition of the polymer formulations as 1 wt.% aqueous solutions (or dispersions) over the sand layer in Petri dishes.

To visualize the stability of a protective coating, Petri dishes with dried polymer-sand samples were placed vertically, and a splitting of sand from the dishes was controlled. Note that, for samples studied, no loss of dried sand was detected (Figure 4a). This result evidences that, in this case, the stable protective coatings or crusts are formed at the sand surface. In all cases, polymer-sand crusts were easily separated from the sand surface as shown in Figure 4b. For comparison, the virgin sand, treated with water and dried, moved to the opposite edge of the dish when the Petri dish was lifted by one edge at an angle of 25 degrees (Figure 4c).

(**a**) (**b**) (**c**)

Figure 4. A Petri dish with sand treated by the W = 0.2 formulation and dried (**a**), the polymer-sand crust took out of the dish (**b**), and a Petri dish with sand treated by water and dried (**c**), reference sample.

The strength of polymer-sand crusts (P_f), quantified by the penetration method, is shown in Table 1 (column 6). The crust composed of sand and virgin BSMs (sample 1, Table 1) is characterized by a low strength P_f = 0.8 MPa. Note that this crust is rather flexible and could be bent to an angle of about 15° without cracking. The saturation of the BSMs surface with PDADMAC chains at W_{sat} = 0.036 results in the growth in strength of the crust to 1.1 MPa (sample 2, Table 1), with the increment Q = dP_f/dW = 8 MPa. Further addition of the cationic PDADMAC to BSMs suspension is accompanied by the noticeable growth in the strength up to 18 Mpa for the crust with a W = 0.5 formulation (sample 8, Table 1). Note that in the 0.059 < W < 0.50 range, polymer-sand crusts demonstrate slight elasticity with the bending angle of 5–7° (samples 3–8, Table 1). The crust based on pure cationic PDADMAC is characterized by the highest strength of 45 MPa (sample 9, Table 1) and well-pronounced brittle fracture under bending.

For a detailed discussion of the influence of composition on the crust strength, let us consider the strength–composition dependence $P_f = f(W)$ (Figure 5a). This dependence demonstrates inflection at the initial portion of the curve. The treatment of this plot in semi-logarithmic coordinates: $P_f = f(\ln W)$ (Figure 5b) showed that this inflection takes place at $\ln W_{in}$ = 2.05, which corresponds to W_{in} = 0.077. An analysis of the results presented in Figure 5 and in Table 1 (column 6) evidences that in the W_{sat} (0.036) < W < W_{in} (0.077) region, the appearance of unbound PDADMAC in the saturated PDADMAC–BSMs complex provided the marked increase of the crust strength with the increment Q = 32 MPa. At W > W_{in}, the efficacy of unbound PDADMAC still grows up to a Q value of 48.

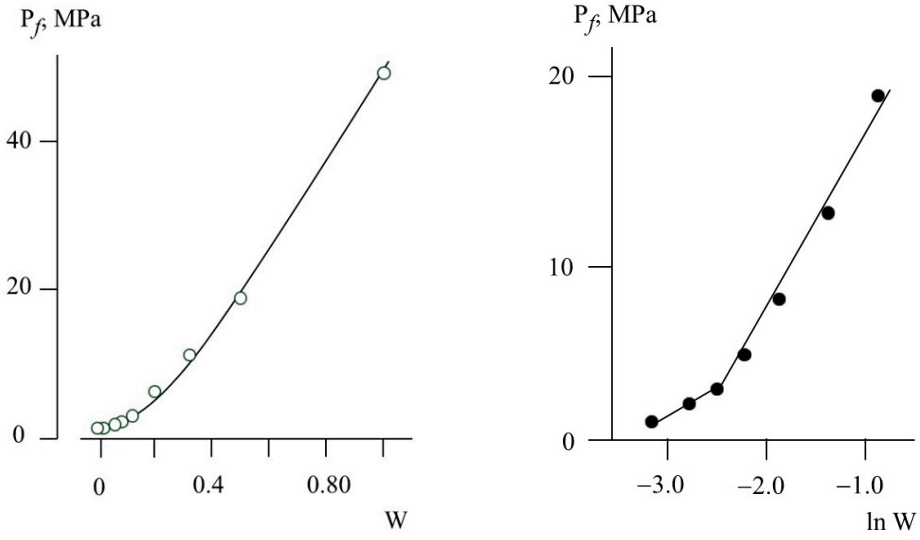

(**a**) (**b**)

Figure 5. Dependence of the strength of polymer-sand crust P_f on the weight fraction of PDADMAC in formulation W (**a**) and ln W (**b**).

Before discussing a possible mechanism of the fixing action of the PDADMAC–BSM mixtures, let us recall an important detail that the sand was always treated with the same amount of the mixtures. In other words, an increase in the PDADMAC content in the mixture was accompanied by a decrease of an equal amount of BSM. Taking into account the above results, the mechanism of the influence of BSMs–PDADMAC formulations on the mechanical properties of polymer-sand crusts can be presented as follows. At W = 0 and W = 0.036, rubbery virgin negatively charged BSMs and positively charged saturated BSMs–PDADMAC systems glue sand particles together. These microscopic events provide the elasticity of the polymer-sand crusts with no marked influence on their strength. At W not higher than 0.077, unbound and free polycation act like an additional glue, thus reinforcing the polymer-sand crust and contributing to strength growth. With an increase in the PDADMAC content within $0.077 < W < 1.0$, the interval unbound PDADMAC chains prevail in the composition. Within this region, the sharp growth in the rigidity of polymer-sand crusts can be attributed to an ability of multi-charged PDADMAC macromolecules to penetrate deeper into the sand sample and to glue more particles in the sand aggregates.

One of the most important operational characteristics of polymer-sand crusts is associated with their water resistance. To estimate this parameter, the crusts were sprayed with water. The removed sand was collected, dried and weighted. The loss of the weight was measured as $S = W_{Sr}/W_{S0} \times 100\%$, where W_{Sr} and W_{S0} are the weights removed and initial sand, respectively (Table 2). The results obtained are evidence that water-resistant crusts are formed when compositions with $0 < W < 0.2$ are used. An increase in PDADMAC content in the formulation is accompanied by the growth in the loss of sand under water spraying.

Table 2. Loss of sand from the polymer-sand crusts prepared with PDADMAC–BSM formulations.

Deposited Formulation	Water (Control)	PDADMAC–BSM Formulation, W				
		0	0.036–0.2	0.333	0.5	1
1	2	3	4	5	6	7
Loss of sand, S, %	30 ± 3	0	0	11 ± 2	19 ± 3	39 ± 5

Hence, the use of BSMs for sand treatment resulted in the formation of low-strength, elastic and water-resistance crust; whereas, the PDADMAC-based crust is characterized by the opposite properties—high strength, brittle and poor water resistance. Obviously, in order to realize the desired combination of operational characteristics of polymer-sand crusts, PDADMAC–BSMs mixtures should be used.

Thus, water-resistant samples with no loss of sand can be prepared at $0 \leq W \leq 0.2$. A further increase in W initiates a removal of sand with water. The correlation of water resistance and PDADMAC content is associated with the fact that an excess of unbound water-soluble PDADMAC is prone to be easily washed out from the inter-particle space of polymer-sand crust. Moreover, PDADMAC results in the hydrophilization of the surface of sand particles enhancing their slippage relative to each other. For these reasons, the accumulation of unbound PDADMAC at $W > 0.2$ decreases the water resistance of the polymer-sand crust and provides a "flow" of moistened polymer-sand composition (Figure 6a); whereas, polymer-sand samples treated by PDADMAC–BSM formulations with $W \leq 0.2$ are stable (Figure 6b). Thus, the variation of PDADMAC content in the formulations allows the control of operational characteristics of a polymer-sand crust.

(**a**) (**b**)

Figure 6. A Petri dish with moistened sand treated by PDADMAC (**a**) and BSM–PDADMAC formulation with W = 0.2 (**b**).

In order to reveal the "structure–property" correlation for the polymer-sand crusts, electron microscopic studies were carried out. Figure 7 shows electron micrographs of the outside surface (a), the edge (b) and transverse fault (c) of the polymer-sand crust. The treatment of sand with the polymer formulations had no significant influence on a sand porous structure (Figure 7a,b). The role of PDADMAC–BSM mixtures is associated with the formation of a polymer film on the sand particle surface, binding them with each other at the points of inter-particle contacts (Figure 7c). The thickness of film was estimated as 0.25–1 μm.

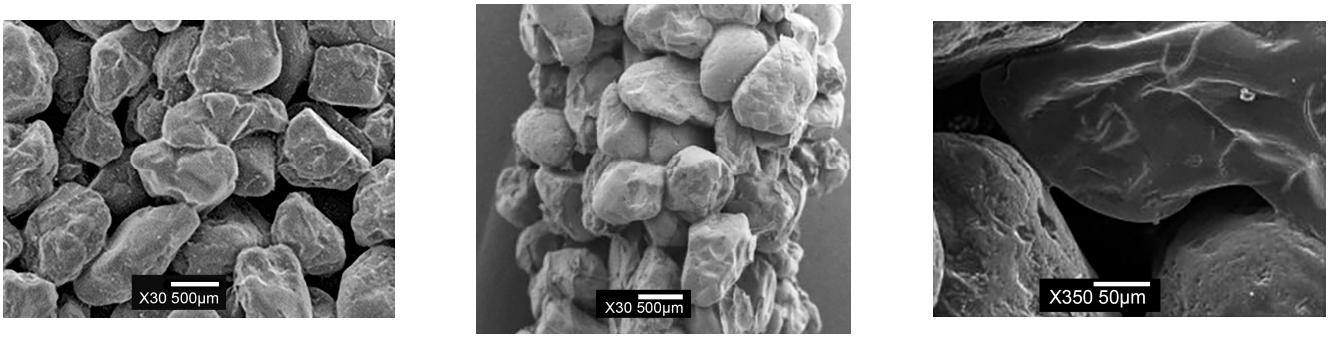

(**a**) (**b**) (**c**)

Figure 7. Micrographs outside the surface (**a**), edge of crust (**b**) and transverse fault (**c**) of the polymer-sand crust prepared with a PDADMAC–BSM formulation (W = 0.2).

4. Conclusions

The mixing of anionic BSMs and aqueous solutions of cationic PDADMAC was accompanied by complexation between these oppositely charged components. At the weight fraction of PDADMAC W = 0.036, the saturated positively charged BSMs–PDADMAC complex was formed. An increase in W up to 0.5 resulted in the accumulation of unbound PDADMAC in aggregately stable BSMs–PDADMAC aqueous formulations.

For the films prepared from the binary BSMs–PDADMAC formulations, with increasing W, the growth in the rigidity of the material (20-fold growth in elastic modulus, 2-fold growth in strength and 2-fold decrease in ultimate strain) was attributed to the accumulation of unbound PDADMAC.

Treatment of the sand with BSMs–PDADMAC formulations is accompanied by polymer binding to sand particles and the formation of ternary BSMs–PDADMAC-sand surface coating (crust) on the soil with porosity comparable to that for the virgin sand. With an increasing weight fraction of PDADMAC from 0 to 1, the growth in the crust strength from 0.8 to 45.0 MPa was observed when crust elasticity was estimated as the bending angle fell down. In parallel to this evolution of the mechanical characteristics, the water-resistance of

the crust decreases. The protective coatings with high strength and water-resistance were shown to be formed at $0.05 < W < 0.2$.

Comparative studies in the mechanical behavior of the binary BSMs–PDADMAC films and ternary BSMs–PDADMAC-sand crusts revealed the following roles of the polymer components: rubbery BSMs contribute to the elasticity of the materials, while unbound PDADMAC controls their rigidity. From this standpoint, the change in weight fraction of PDADMAC allowed one to control "rigidity–elasticity" balance of both polymer-colloid films and sand surface coatings.

Electron microscopic studies of polymer-sand crusts evidenced the following "structure–property" correlation for them. The treatment of sand with the BSMs–PDADMAC formulations does not influence a sand porous structure, and the role of the polymeric binder is associated with the appearance of the polymer film on the surface of the sand particle with the thickness of 0.25–1 μm. The latter factor is responsible for the binding of sand particles with each other at the points of inter-particle contacts. In other words, the formation of a strong polymer-sand crust is associated with the binding of sand particles by polymeric "bridges" with no influence on the porous sand structure.

These observations can be supplemented by the literature data on the stability of ionic polymers which are the initial components of the stabilizing IPEC formulations. The shelf life of polymers and the relevant IPECs have been actively tested previously. Particularly, the long-term stability for the initial polymers was shown under different weather conditions (frost, hot weather, rain and etc.) [53,54]. Polymer-soil coatings withstood multiple repeated freezing–thawing and wetting–drying cycles. However, these works were mainly carried out with linear polymers, which, being bonded to soil and sand, form rather rigid coatings. This approach has proved to be excellent when treating vast flat areas, such as fields, slopes of wide ravines, etc. Problems appear when these conventional formulations are used for stabilizing sites with a more complicated relief, e.g., decorative zones and open-air museums. In this case, different formulations are required which are capable of forming elastic coatings and which maintain integrity for a long time. As follows, from the above, the elasticity of the polymer-soil coating can be increased via using latex, an aqueous suspension of rubbery polymeric microspheres. Additionally, synthetic ionic polymers were shown to demonstrate a negligible toxicity towards soil microorganisms and higher plants after these polymers bind to soil and sand [44]. From here, the aqueous latex–PDADMAC polycomplexes can be recommened as promising binders for soil and sand which form elastic and biocompatible surface coatings. The latex-based IECs together with earlier described conventional IPECs, composed of linear ionic polymers, represent a family of universal binders whose properties can be easily adapted to specific conditions of areas to be treated.

Author Contributions: Conceptualization, A.Y. and I.P.; methodology, I.P. and M.A.; software, I.G.; validation, I.G. and M.A.; formal analysis, A.Y.; investigation, E.S.; resources, A.Y.; data curation, I.G. and A.Y.; writing—original draft preparation, I.P.; writing—review and editing, A.Y.; visualization, I.P. and M.A.; supervision, A.Y.; project administration, I.P.; funding acquisition, A.Y. All authors have read and agreed to the published version of the manuscript.

Funding: This research was funded by the Russian Science Foundation, grant number 22-13-00124 (https://rscf.ru/en/project/22-13-00124/ accessed on 1 January 2023).

Institutional Review Board Statement: Not applicable.

Informed Consent Statement: Not applicable.

Data Availability Statement: Not applicable.

Conflicts of Interest: The authors declare no conflict of interest.

References

1. Shen, J.; Liang, J.; Lin, X.; Lin, H.; Yu, J.; Yang, Z. Recent progress in polymer-based building materials. *Int. J. Polym. Sci.* **2020**, *2020*, 8838160. [CrossRef]
2. Darwish, M.S.; Mostafa, M.H.; Al-Harbi, L.M. Polymeric Nanocomposites for Environmental and Industrial Applications. *Int. J. Mol. Sci.* **2022**, *23*, 1023. [CrossRef]
3. Huang, J.; Kogbara, R.B.; Hariharan, N.; Masad, E.A.; Little, D.N. A state-of-the-art review of polymers used in soil stabilization. *Constr. Build. Mater.* **2021**, *305*, 124685. [CrossRef]
4. Halliwell, S.M. *Polymers in Building and Construction*; Rapra Technology: Shrewsbury, UK, 2003.
5. Lu, Y.; Shah, K.W.; Xu, J. Synthesis, morphologies and building applications of nanostructured polymers. *Polymers* **2017**, *9*, 506. [CrossRef]
6. Zhang, X.; Du, M.; Fang, H.; Shi, M.; Zhang, C.; Wang, F. Polymer-modified cement mortars: Their enhanced properties, applications, prospects, and challenges. *Constr. Build. Mater.* **2021**, *299*, 124290. [CrossRef]
7. Li, X.; Liu, R.; Li, S.; Zhang, C.; Li, J.; Cheng, B.; Liu, Y.; Ma, C.; Yan, J. Effect of SBR and XSBRL on water demand, mechanical strength and microstructure of cement paste. *Constr. Build. Mater.* **2022**, *332*, 127309. [CrossRef]
8. Behnood, A.; Gharehveran, M.M. Morphology, rheology, and physical properties of polymer-modified asphalt binders. *Eur. Polym. J.* **2019**, *112*, 766–791. [CrossRef]
9. Habbouche, J.; Hajj, E.Y.; Sebaaly, P.E.; Piratheepan, M. A critical review of high polymer-modified asphalt binders and mixtures. *Int. J. Pavement Eng.* **2020**, *21*, 686–702. [CrossRef]
10. Yamaguchi, A.; Kanashiki, N.; Ishizaki, H.; Kobayashi, M.; Osawa, K. Relationship between soil erodibility by concentrated flow and shear strength of a Haplic Acrisol with a cationic polyelectrolyte. *Catena* **2022**, *217*, 106506. [CrossRef]
11. Panova, I.G.; Ilyasov, L.O.; Yaroslavov, A.A. Polycomplex formulations for the protection of soils against degradation. *Polym. Sci. Ser. C* **2021**, *63*, 237–248. [CrossRef]
12. Latifi, N.; Horpibulsuk, S.; Meehan, C.L.; Abd Majid, M.Z.; Tahir, M.M.; Mohamad, E.T. Improvement of problematic soils with biopolymer—An environmentally friendly soil stabilizer. *J. Mater. Civ. Eng.* **2017**, *29*, 04016204. [CrossRef]
13. Zhang, J.; Yi, W.; Yuan, W.; Liu, Y.; Sui, Z. Research on the Ecological Protection of Coal Gangue Slope Based on a Polymer Curing Agent. *Adv. Mater. Sci. Eng.* **2021**, *2021*, 8181688. [CrossRef]
14. Yang, Y.; Wei, Z.; Dong, X.; Lu, T.; Chen, Y.; Wang, W. Experimental study on the mechanical properties of polymer-treated tailings. *Arab. J. Geosci.* **2021**, *14*, 2653–2666. [CrossRef]
15. Li, F.; Wang, C.; Xia, Y.; Hao, Y.; Zhao, P.; Shi, M. Strength and Solidification Mechanism of Silt Solidified by Polyurethane. *Adv. Civ. Eng.* **2020**, *2020*, 8824524. [CrossRef]
16. Li, R.; Zhang, B.; Wang, Y.; Zhao, Y.; Li, F. Leaching potential of stabilized fly ash from the incineration of municipal solid waste with a new polymer. *J. Environ. Manag.* **2019**, *232*, 286–294. [CrossRef]
17. Yang, Q.W.; Pei, X.J.; Huang, R.Q. Impact of polymer mixtures on the stabilization and erosion control of silty sand slope. *J. Mt. Sci.* **2019**, *16*, 470–485. [CrossRef]
18. Li, T.; Dai, F.; He, Y.; Xu, D.; Wang, R. An Eco-Friendly Polymer Composite Fertilizer for Soil Fixation, Slope Stability, and Erosion Control. *Polymers* **2022**, *14*, 1461. [CrossRef]
19. Liang, Y.; Yeh, T.-C.J.; Ma, C.; Zhang, J.; Xu, W.; Yang, D.; Hao, Y. Experimental investigation on hole erosion behaviors of chemical stabilizer treated soil. *J. Hydrol.* **2020**, *594*, 125647. [CrossRef]
20. Zang, Y.X.; Gong, W.; Xie, H.; Liu, B.L.; Chen, H.L. Chemical sand stabilization: A review of material, mechanism, and problems. *Environ. Technol. Rev.* **2015**, *4*, 119–132. [CrossRef]
21. Zinchenko, A.; Sakai, T.; Morikawa, K.; Nakano, M. Efficient stabilization of soil, sand, and clay by a polymer network of biomass-derived chitosan and carboxymethyl cellulose. *J. Environ. Chem. Eng.* **2022**, *10*, 107084. [CrossRef]
22. Xu, G.; Ding, X.; Kuruppu, M.; Zhou, W.; Biswas, W. Research and application of non-traditional chemical stabilizers on bauxite residue (red sand) dust control, a review. *Sci. Total Environ.* **2018**, *616*, 1552–1565. [CrossRef]
23. Alakbari, F.S.; Mohyaldinn, M.E.; Muhsan, A.S.; Hasan, N.; Ganat, T. Chemical sand consolidation: From polymers to nanoparticles. *Polymers* **2020**, *12*, 1069. [CrossRef]
24. Koohestani, B.; Darban, A.K.; Mokhtari, P.; Darezereshki, E.; Yilmaz, E. Geopolymerization of soil by sodium silicate as an approach to control wind erosion. *Int. J. Environ. Sci. Technol.* **2021**, *18*, 1837–1848. [CrossRef]
25. Porter, H.; Dhami, N.K.; Mukherjee, A. Synergistic chemical and microbial cementation for stabilization of aggregates. *Cem. Concr. Compos.* **2017**, *83*, 160–170. [CrossRef]
26. James, J.; Vijayasimhan, S.; Eyo, E. Stress-Strain Characteristics and Mineralogy of an Expansive Soil Stabilized Using Lime and Phosphogypsum. *Appl. Sci.* **2023**, *13*, 123. [CrossRef]
27. Yi, H.; Oh, K.; Kou, R.; Qiao, Y. Sand-filler structural material with a low content of polyethylene binder. *Sustain. Mater. Technol.* **2020**, *25*, e00194. [CrossRef]
28. Song, Z.; Liu, J.; Bai, Y.; Wei, J.; Li, D.; Wang, Q.; Qian, W. Laboratory and field experiments on the effect of vinyl acetate polymer-reinforced soil. *Appl. Sci.* **2019**, *9*, 208. [CrossRef]
29. Mirzababaei, M.; Arulrajah, A.; Horpibulsuk, S.; Soltani, A.; Khayat, N. Stabilization of soft clay using short fibers and polyvinyl alcohol. *Geotext. Geomembr.* **2018**, *46*, 646–655. [CrossRef]

30. Sojka, R.E.; Bjorneberg, D.L.; Entry, J.A.; Lentz, R.D.; Orts, W.J. Polyacrylamide in agriculture and environmental land management. *Adv. Agron.* **2007**, *92*, 75–162.
31. Saleh, S.; Yunus, N.Z.M.; Ahmad, K.; Ali, N. Improving the strength of weak soil using polyurethane grouts: A review. *Constr. Build. Mater.* **2019**, *202*, 738–752. [CrossRef]
32. Albalasmeh, A.A.; Hamdan, E.H.; Gharaibeh, M.A.; El Hanandeh, A. Improving aggregate stability and hydraulic properties of Sandy loam soil by applying polyacrylamide polymer. *Soil Tillage Res.* **2021**, *206*, 104821. [CrossRef]
33. Kumar, P.; Puppala, A.J.; Tingle, J.S.; Chakraborty, S.; Sarat Chandra Congress, S. Resilient Characteristics of Polymer Emulsion-Treated Sandy Soil. *Transp. Res. Rec.* **2022**, *2676*, 526–538. [CrossRef]
34. Baghini, M.S.; Ismail, A.; Naseralavi, S.S.; Firoozi, A.A. Performance evaluation of road base stabilized with styrene–butadiene copolymer latex and Portland cement. *Int. J. Pavement Res. Technol.* **2016**, *9*, 321–336. [CrossRef]
35. Lu, S.; Wang, Z.; Hu, Y.; Liu, B.; Liu, J.E. Effectiveness and durability of polyacrylamide (PAM) and polysaccharide (Jag C 162) in reducing soil erosion under simulated rainfalls. *Water* **2018**, *10*, 257. [CrossRef]
36. Lentz, R.D. Polyacrylamide and biopolymer effects on flocculation, aggregate stability, and water seepage in a silt loam. *Geoderma* **2015**, *241–242*, 289–294. [CrossRef]
37. Ahbab, A.; Sardroud, S.N.E.; Katebi, H.; Avci, E. Prevention of Wind Erosion in Salty Lands of Urmia Lake with Butadiene Carboxylic Latex and Cement Grout. *Iran. J. Sci. Technol. Trans. Civ. Eng.* **2022**, *47*, 447–455. [CrossRef]
38. Liu, J.; Bai, Y.; Song, Z.; Lu, Y.; Qian, W.; Kanungo, D.P. Evaluation of strength properties of sand modified with organic polymers. *Polymers* **2018**, *10*, 287. [CrossRef]
39. Arias-Trujillo, J.; Matías-Sanchez, A.; Cantero, B.; López-Querol, S. Effect of polymer emulsion on the bearing capacity of aeolian sand under extreme confinement conditions. *Constr. Build. Mater.* **2020**, *236*, 117473. [CrossRef]
40. Izumrudov, V.A.; Mussabayeva, B.K.; Kassymova, Z.S.; Klivenko, A.N.; Orazzhanova, L.K. Interpolyelectrolyte complexes: Advances and prospects of application. *Russ. Chem. Rev.* **2019**, *88*, 1046. [CrossRef]
41. Kabanov, V.A. Polyelectrolyte complexes in solution and in bulk. *Russ. Chem. Rev.* **2005**, *74*, 3–20. [CrossRef]
42. Klivenko, A.; Orazzhanova, L.; Mussabayeva, B.; Yelemessova, G.; Kassymova, Z. Soil structuring using interpolyelectrolyte complexes of water-soluble polysaccharides. *Polym. Adv. Technol.* **2020**, *31*, 3292–3301. [CrossRef]
43. Novoskoltseva, O.A.; Loiko, N.G.; Nikolaev, Y.A.; Lisin, A.O.; Panova, I.G.; Yaroslavov, A.A. Interpolyelectrolyte complexes based on hydrolyzed polyacrylonitrile for anti-erosion stabilization of soils and ground. *Polym. Int.* **2022**, *71*, 697–705. [CrossRef]
44. Yakimenko, O.; Ziganshina, A.; Terekhova, V.; Panova, I.; Gladkova, M.; Timofeev, M.; Yaroslavov, A. Ecotoxicity of polyelectrolyte formulations in water and soil matrices. *Environ. Sci. Pollut. Res.* **2022**, *29*, 65489–65499. [CrossRef]
45. George, S.C.; Ninan, K.N.; Groeninckx, G.; Thomas, S. Styrene–butadiene rubber/natural rubber blends: Morphology, transport behavior, and dynamic mechanical and mechanical properties. *J. Appl. Polym. Sci.* **2000**, *78*, 1280–1303. [CrossRef]
46. Alimardani, M.; Abbassi-Sourki, F. New and emerging applications of carboxylated styrene butadiene rubber latex in polymer composites and blends: Review from structure to future prospective. *J. Compos. Mater.* **2015**, *49*, 1267–1282. [CrossRef]
47. Khaidapova, D.D.; Pestonova, E.A. Strength of interparticle bonds in soil pastes and aggregates. *Eurasian J. Soil Sci.* **2007**, *40*, 1187–1192. [CrossRef]
48. Sukhishvili, S.A.; Chechik, O.S.; Yaroslavov, A.A. Adsorption of poly-N-ethyl-4-vinylpyridinium bromide on the surface of carboxylated latex particles: Composition and structure of interfacial complex. *J. Colloid Interface Sci.* **1996**, *178*, 42–46. [CrossRef]
49. Bauer, D.; Buchhammer, H.; Fuchs, A.; Jaeger, W.; Killmann, E.; Lunkwitz, K.; Rehmet, R.; Schwarz, S. Stability of colloidal silica, sikron and polystyrene latex influenced by the adsorption of polycations of different charge density. *Colloids Surf. A Physicochem. Eng. Asp.* **1999**, *156*, 291–305. [CrossRef]
50. Choi, J.; Rubner, M.F. Influence of the degree of ionization on weak polyelectrolyte multilayer assembly. *Macromolecules* **2005**, *38*, 116–124. [CrossRef]
51. Szilagyi, I.; Trefalt, G.; Tiraferri, A.; Maroni, P.; Borkovec, M. Polyelectrolyte adsorption, interparticle forces, and colloidal aggregation. *Soft Matter* **2014**, *10*, 2479–2502. [CrossRef]
52. Kleimann, J.; Gehin-Delval, C.; Auweter, H.; Borkovec, M. Super-stoichiometric charge neutralization in particle− polyelectrolyte systems. *Langmuir* **2005**, *21*, 3688–3698. [CrossRef]
53. Li, H.; Cui, C.; Temitope, A.A.; Feng, Z.; Zhao, G.; Guo, P. Effect of SBS and crumb rubber on asphalt modification: A review of the properties and practical application. *J. Traffic Transp. Eng.* **2022**, *9*, 836–863. [CrossRef]
54. Borthakur, A.; Das, T.K.; Zhang, Y.; Libbert, S.; Prehn, S.; Ramos, P.; Dooley, G.; Blotevogel, J.; Mahendra, S.; Mohanty, S.K. Rechargeable stormwater biofilters: In situ regeneration of PFAS removal capacity by using a cationic polymer, polydiallyldimethylammonium chloride. *J. Clean. Prod.* **2022**, *375*, 134244. [CrossRef]